

# Matching Fingerprints with a Toroidal Iterative Closest Point Algorithm

COURTNEY R. PITCHER, University of Cape Town, South Africa

PATRICK C. MARAIS, University of Cape Town, South Africa

LUKE N. DARLOW, School of Informatics, University of Edinburgh, Scotland, United Kingdom

We develop a generalisable Cartesian-toroidal Iterative Closest Points (ICP) fingerprint matcher. Both 2D and 3D minutiae are cast as point clouds that we augment with additional features. ICP is immediately applicable to these data structures, yet nonetheless relatively unexplored in the fingerprinting domain. We apply our ICP-based method to conventional 2D minutiae and 3D features extracted from Optical Coherence Tomography (OCT) scans of fingertips. We show that ICP is a viable strategy to fingerprint matching using the diverse features in the internal fingerprint skin. Using 3D minutiae alone gave an Area Under the Curve (AUC) of 0.961, and 3D minutiae augmented with mean local OCT intensity gave an AUC of 0.973. Regarding 2D minutiae, our method offers a significant improvement over the baseline NIST *Bozorth3* algorithm: an AUC of 0.94 versus 0.86 on an artificial dataset generated with *SFinGe*. In addition, ICP incurs only nominal computation cost when additional features are added.

CCS Concepts: • **Security and privacy** → **Biometrics**; **Access control**;

Additional Key Words and Phrases: biometrics, 3D fingerprint matching, fingerprint matching, ICP, 3D features

## 1 INTRODUCTION

Biometrics are ubiquitous components of many security and identification systems, and fingerprints are the most commonplace biometric owing to their non-invasive acquisition and acceptance. Traditionally, fingerprinting was defined as the study of patterns in the frictional ridge skin on the surface of the fingertip. A typical feature type is a minutia, the points in the ridges of the frictional ridge skin where a ridge either terminates or splits. These features are usually extracted from the fingerprint by pressing the fingerprint against a 2D optical scanner or inked paper. In 2D the structures are represented by the tuple  $(x, y, \theta)$ , where the first two elements are the position and the last is the orientation of the ridgeline. In 3D these structures are represented by the tuple  $(x, y, z, \theta, \varphi)$ , where the first three elements are the Cartesian location, followed by the polar and azimuthal angles respectively (tangent to the ridgeline in 3D). Minutiae are an inherently 3D structure that is flattened, and therefore distorted when captured in 2D.

Optical Coherence Tomography (OCT) is an emerging scanning technology that uses low-energy laser pulses to image the internal skin, thereby providing richer information content than other 3D imaging [6]. These scans allow richer and more complex features to be extracted from the finger, such as microstructures within the tissue of the fingertip. They also offer the possibility of extracting the internal fingerprint, which is at the junction between the

---

dermis and epidermis and is a near copy of the surface (external) fingerprint. The external fingerprint is prone to degradation due to a variety of causes, including weathering, scratching, ageing, and birth defects. As the internal fingerprint is not as susceptible to these kinds of damage, biometric systems that use this layer are more attractive.

Given the emergence of 3D OCT scanners, and the continued widespread use of 2D fingerprinting, a fingerprint matching system that supports feature matching under either regime would be of great use. A robust general point matching scheme, widely used in computer vision, is ICP. However, ICP is not directly applicable to fingerprinting: the simplest fingerprinting feature, 2D minutia, are composed of a Cartesian  $(x, y)$  position and *rotation*. The rotation is an element of a toroidal space which is incompatible with the standard Cartesian ICP implementation. ICP was designed to align Cartesian coordinates [1]. Cartesian metrics produce spurious results in toroidal space, e.g. the angular distance between  $10^\circ$  and  $350^\circ$  is  $20^\circ$  and not  $340^\circ$ .

In this paper, we develop a Cartesian-toroidal ICP feature matcher and show how this can be used to accurately and quickly match fingerprints in both 2D and 3D. In addition to the standard 2D features, we also introduce appropriate low-cost 3D features that contain sufficient information for robust and fast matching. To avoid confusion we name this matcher Fingerprint ICP (FICP).

This paper is laid out as follows: Section 2 outlines previous work in this area. The features and their method of extraction are described in Section 3. Section 4 details the FICP matcher and modifications for the features described in the previous section. Section 5 shows the results and the datasets used to obtain them. The conclusion and future work are presented in Section 6.

## 2 RELATED WORK

Kumar and Kwong propose a 3D minutiae extractor that extracts the features using principal curvature calculated on the entire finger surface cloud [9]. Our extractor requires the curvature to be calculated in a small Region of Interest (ROI) around each 2D minutia, which is less expensive.

Bhowmick et.al. show  $k$ -d trees to be an effective means to match and store 2D minutiae [2]. Our matcher and storage is distinct from this method in that we store the toroidal component in a toroidal space, we aggregate the feature difference into a single value, and we match the toroidal spaces with a more appropriate and lower cost metric.

## 3 FEATURE EXTRACTION

We tested our system with three feature types: 2D minutiae, 3D minutiae, and 3D minutiae with mean local intensities.

### 3.1 2D Minutiae

The 2D minutiae were extracted from the *SFinGe* fingerprint images using *MINDTCT* [12], see Figure 1c. This feature extractor was chosen as it is an open-source, well-optimised baseline. To simulate a scan, 50% of the minutiae were randomly discarded, a translation noise of  $[-10..10]$  pixels and an angular noise of  $[-10..10]$  degrees were applied to each minutia, a global translation of  $[0..100]$  pixels was applied in a random direction, and a global rotation of  $[-20..20]$  degrees was applied. The chosen distortion values simulate scans that are of sufficiently poor quality to demonstrate the lower bound of matching performance, see Figure 5 for robustness with poor data. A second scan was simulated for each fingerprint using the same process, see Figure 1d. This yields a total of 12 500 scans, two per fingerprint. This distortion might be considered severe, but it shows the matcher’s good performance with low-quality data and its resilience to rotation, translation, and noise.

### 3.2 3D Minutiae

The 3D minutiae are extracted from the internal fingerprint surface in the OCT scans using the extraction pipeline described in below. Before extraction begins, a flattened 2D internal fingerprint is extracted from the OCT volume using the method by Darlow et. al. [4].

*MINDTCT* is used to extract 2D minutiae from the flattened internal fingerprint. We developed a scheme to translate the 2D minutiae into 3D. The scheme uses the 2D minutiae locations as Points of Interest (POIs) for extracting 3D minutiae. The 2D minutiae are distorted and the nearest 3D point (on the internal fingerprint surface) cannot be used as the position of the 3D minutiae. Consequently, the first step is to find the true apex of the ridge, where the minutia should be located. For each 2D minutia, a group of points – ROI – is found in the cloud with a similar  $x$  and  $y$  coordinate to that of the minutia. Starting from the centre of the ROI and working outwards, the normal curvature of each point is calculated. The closest point to the 2D minutia with a maximum curvature close to 0 and a maximum curvature vector aligned with the 2D minutia’s azimuthal angle is chosen to be the 3D minutia. The position is the minutia’s Cartesian component and the maximum curvature eigenvector is the orientation. If the point is umbilic, a tangent vector that is the result of projecting the 2D minutia’s azimuthal angle on to the tangent plane is used instead of the maximum curvature vector.

The simultaneous extraction of 2D and 3D minutiae is a useful by-product, that has been shown to be a useful composite feature [9].

### 3.3 3D Minutiae with Mean Local Intensity

There may be features at points other than the internal fingerprint surface. These include secondary biometric features, such as sweat glands. These features may not be easily discernible in low-quality scans, but they will appear as regions of higher and lower density. We can thus approximate these secondary features by calculating the *mean local intensity* in a spherical ROI, around a given location (point of interest). This is simply the average of the voxel intensities in the given ROI. This feature is represented by the tuple  $(x, y, z, \theta, \phi, i)$ , where  $i$  is the mean intensity. The OCT volume is an organised point cloud, i.e. matrix, so neighbouring intensity searches are cheap.

## 4 ITERATIVE CLOSEST POINT MATCHER

ICP is designed to align two corresponding *point clouds*. It works by iteratively: (1) finding corresponding points in the two clouds, (2) estimating the combination of rotation and translation to minimise the distance between those corresponding points, and (3) applying the transformation to the first cloud.

ICP requires a function to find corresponding points between the two clouds being matched. To do this, a real number distance must be calculated in the feature space. To find the distance between two Cartesian coordinates in  $\mathbb{R}^n$ , the Euclidean distance suffices. Unfortunately, as noted earlier, we have extracted features that are not entirely in  $\mathbb{R}^n$ . *We thus develop a custom metric to find corresponding features in this more complex feature space.*

To construct this metric each coordinate subspace is assigned a weighting. The position is always assigned a weight of 1, whereas the other coordinate subspaces are assigned experimentally derived weights. The weighting parameters aggregate the Cartesian and toroidal components into the single real number required for the feature metric. The weighting represents the relative importance of orientation to the other members of the feature.

As a preprocessing step, all orientations are converted to orientation quaternions, so that they can be measured with the metric  $1 - |q_1 \cdot q_2|$ . The quaternion inner product metric describes the angular displacement with a single real

number in the range  $[0, 1]$ , furthermore, it has an inverted cosine shape, which biases it to minutiae it partially aligns with. As opposed to an Euclidean distance which has a sine shape and is biased in the opposite direction. This metric has a low time complexity, requiring only four multiplications and one comparison to compute [7].

The metric for minutiae,  $D(A, B)$ , is as follows:

$$D_1(A, B) = d(A_{x,y,z}, B_{x,y,z}) + \alpha(1 - |A_q \cdot B_q|), \quad (1)$$

where  $A$  and  $B$  are minutiae,  $d()$  is the Euclidean metric,  $\alpha$  is the weight for the toroidal dimension(s), and  $A_q$  and  $B_q$  are the orientation of the minutiae represented as quaternions.

The metric for composite minutiae and mean local intensity,  $D(A, B)$ , is as follows:

$$D_2(A, B) = D_1(A, B) + \beta|A_i - B_i|, \quad (2)$$

where  $A$  and  $B$  are the composite features,  $\beta$  is the weight for the local intensity, and  $A_i$  and  $B_i$  are intensities. Cartesian weightings, such as  $\beta$  can be applied to the dimension before matching occurs.

These metrics condense the spatial difference and angular displacement into two separate variables. These two differences can be aggregated into a single value after a weighting has been applied. This approach allows a match to be scored on the sum of its feature space distances between aligned pairs of features. This is a single threshold that determines whether features matched or not, as opposed to using a threshold per feature dimension [9].

We implemented toroidal  $k$ -d trees to store the features, which have a search time of  $O(\log n)$  as opposed to a linear search which is  $O(n)$ .

## 5 RESULTS AND DISCUSSION

We use two datasets to test our FICP matcher (Section 5.1) on generated 2D fingerprints (Section 5.2) and 3D OCT fingerprints (Section 5.3). We also test the matcher’s resilience to poor quality data (Section 5.4).

### 5.1 Datasets

The FICP matcher is tested on two datasets to demonstrate its utility for both existing and emerging technologies:

- Artificially generated fingerprints using the Synthetic Fingerprint Generator - *SFinGe* [3] for testing FICP applied to conventional **2D minutiae**;
- OCT volume scans to test the matcher on extended **3D features**.

*2D Fingerprints.* The goal of this research is to demonstrate the capabilities of a feature matcher, and not an extractor. Therefore, we used an artificial fingerprint generator to reduce any confounding minutiae extraction error. The dataset consists of synthetic 2D fingerprints of each combination of the five fingers (i.e. thumb, index, middle, ring, and pinky) and the five major fingerprint pattern types (i.e. arches, left loops, right loops, tented arches, and whorls). Each of these 25 combinations has 250 fingerprints, totalling 6250 fingerprints. The resolution of each image is  $656 \times 800$  pixels. These fingerprints were generated without scanner simulation, Figure 1 shows an example of these synthetic fingerprints.

*3D Fingerprints.* The 3D point clouds were captured by a Thorlabs OCS1300SS OCT scanner at two different resolutions [5]. There are a total of 90 scans, all with a depth of 512 voxels. The scans are evenly divided between two  $X - Y$  resolutions of  $256^2$  at 500 dpi, and  $512^2$  at 867 dpi. The fingers were scanned at roughly the same alignment. This is a consequence of how a subject is scanned in an OCT scanner, and ensures that the scans are all partially pre-aligned.

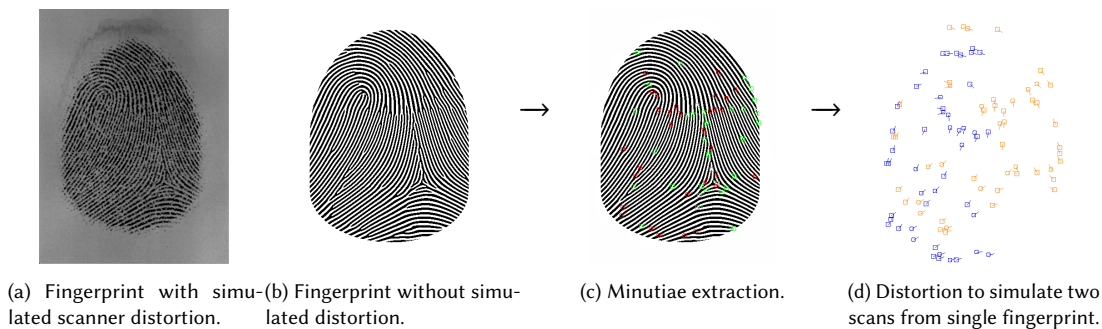


Fig. 1. These images are generated with *SFinGe* [3]. First is the result of emulating scanning and simulating skin distortion such as wear and scratches. The second image is the same fingerprint, but has not been passed through *SFinGe*'s distortion pipeline and constitute the data we used. The third image shows the ground truth minutiae, extracted from the second image using *MINDTCT*. The fourth image shows the artificial distortion of the minutiae to simulate two separate scans of the fingerprint.

Since OCT scanners are still expensive [8] and not widely available, only a small set of scans could be sourced.

OCT scanners capture a region of skin as a volume of voxels with corresponding intensity representing how much energy was reflected back at the scanner. This scan is stored as a 4D organised point cloud (matrix) of  $(x, y, z, i)$ , where the first three elements are the Cartesian location and the last element is the voxel's intensity.

The OCT dataset was downsampled to resolution of  $256^3$  voxels using Point Cloud Library's (PCL) VoxelGrid method, which maintains the voxel cube structure of the scans. The point clouds were downsampled to decrease the processing time, and increase the signal to noise ratio. Quicker processing time is vital in human facing applications of this technology. Although downsampling reduces the level of detail, the gains outweigh the cost, and downsampling is often a part of biometric systems [10].

## 5.2 Matching with 2D Features

We organised the dataset into six experiment categories: arch, left loop, right loop, tented arch, whorl, and all. The first five categories test FICP as if a pre-matching step was performed to ensure match candidates are in the same family. This is typical of many fingerprinting pipelines. The last category tests on the entire dataset without partitioning, simulating no pre-matching step.

An initialisation experiment was performed to find the optimal angle coefficient value,  $\alpha$ , for each experiment category. 8% of the fingerprints were used to perform parameter optimisation, leaving 1150 pairs of matching scans of each pattern type to be used for the matching experiments. An equal number of non-matching scans were randomly chosen from the same dataset category.  $\alpha$  values from 0 to 20, with 0.1 increments, were evaluated via AUC. The  $\alpha$  value that yielded the greatest difference in errors was chosen for the main experiments. The values for the experiment categories are 1.1, 4.7, 4.9, 1.9, 2.9, and 4.2 respectively. The optimal  $\alpha$  values produced a smaller change in AUCs than in 3D matching.

The matcher was tested on an equal number of matching pairs and non-matching pairs of scans. These pairs were chosen from the same dataset category. For the fingerprint family category, a non-matching scan was chosen from the same family, whereas in the "all" category the scan was chosen randomly from the entire dataset. Figure 2 shows the Receiver Operating Characteristic (ROC) for all six experiment categories. For all the graphs our FICP matcher is superior to Bozorth3 in terms of AUC. The FICP matcher dominates the Bozorth3 matcher for arches, right loops,

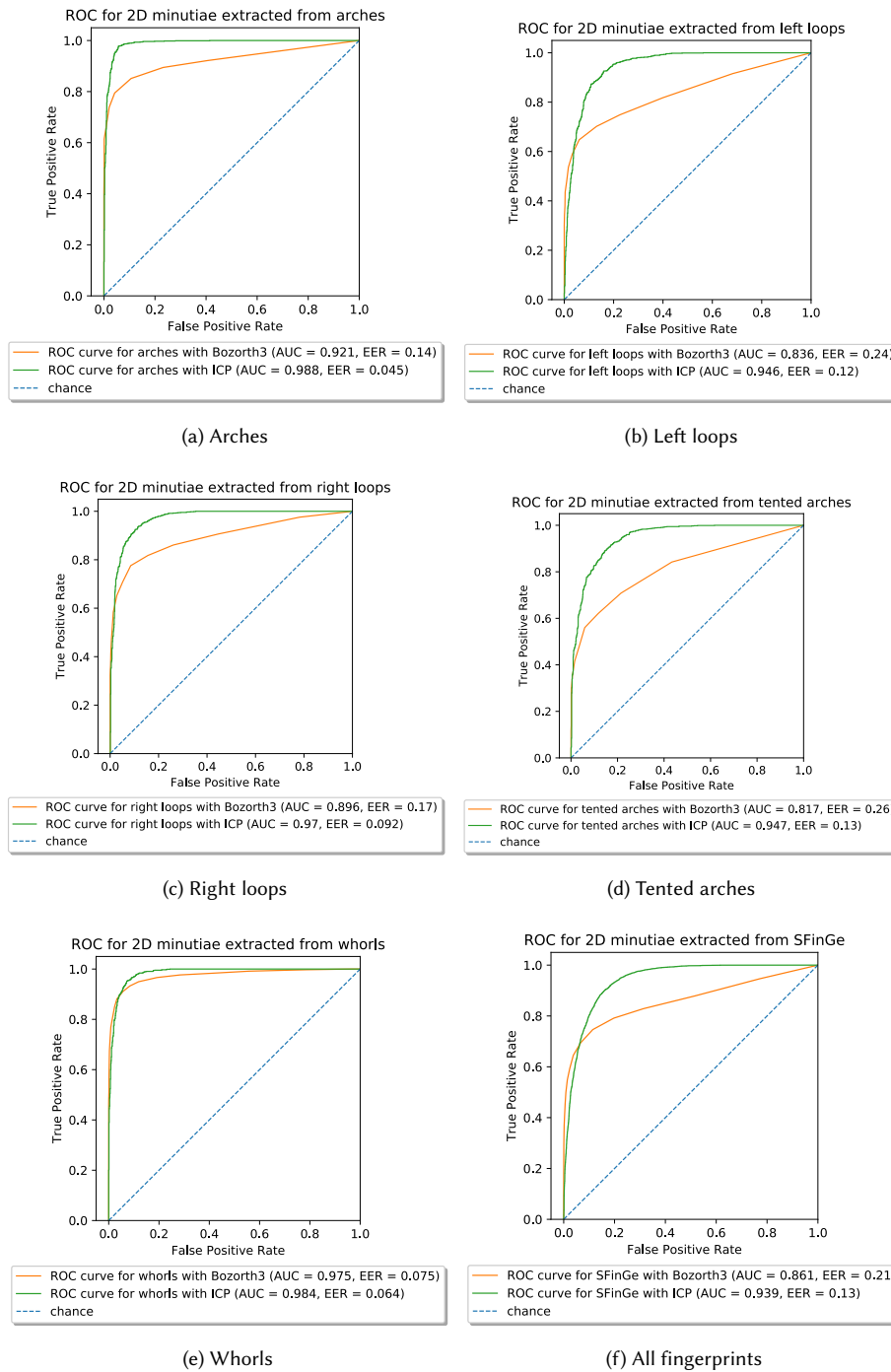


Fig. 2. The above figures illustrate the effectiveness of FICP over Bozorth3. All the data used for these results was generated with the SFinGe tool [3].

and tented arches; see Figures 2a, 2c, and 2d respectively. Whorls produced the smallest difference in AUC, although this was due to the relatively high performance of Bozorth3 on this datatype, see Figure 2e. FICP produced a fairly consistent AUC for each datatype, ranging from 0.946 to 0.988; while Bozorth3 had a more variable AUC range of 0.817 to 0.975. The Bozorth3 matcher ROC curves are skewed towards high specificity and are therefore better at predicting the positive case. While the ROC curves for the FICP matcher were nearly uniform with a small bias towards high sensitivity and are slightly better at predicting the negative case. This makes FICP better in security applications, such as access control, where false positives are undesirable. For all the results shown in Figure 2, FICP will either have a higher True Positive Rate (TPR) for low False Positive Rate (FPR) values ( $FPR < 0.1$ ) of a very similar TPR. At very high TPR values ( $TPR > 0.9$ ), FICP is always superior to Bozorth3 in terms of FPR.

The time required to match the scans was recorded. The 95% confidence interval for the *Bozorth3* matcher is  $12.3 \pm 0.179$  (1.5%) milliseconds, whereas FICP is  $29.2 \pm 0.327$  (1.1%) milliseconds. Our FICP implementation is written in Python3 with Numpy, which is limited to a single core. The test machine’s CPU is an Intel core i7-3820 clocked at 3.8 GHz. ICP is embarrassingly parallel, as a result an optimised multi-core CPU or GPU implementation will perform substantially better. *Bozorth3* is an optimised, mature matcher.

### 5.3 Matching 3D Features

As with the 2D experiments, the dataset was partitioned for parameter optimisation experiments. In both cases, a third of the matching scans and an equal number of non-matching scans are used to determine the best matching parameters. The 3D minutiae have an  $\alpha$  value that combines the angular component with the Cartesian component. The composite 3D minutiae with mean local intensity have an additional  $\beta$  parameter to aggregate the mean local intensity. The best  $\alpha$  value for 3D minutiae was chosen by running the optimisation experiment with every value between 0 and 20, with 0.1 increments. For the composite feature this was done for both parameters ( $\alpha$  and  $\beta$ ) dependently, yielding 40 000 parameter combination experiments. The best parameter values ( $\alpha = 9.4$ ,  $\beta = 1.1$ ) are used for the results in this section.

The AUCs for different values of  $\alpha$  for 3D minutiae are shown in Figure 3. An angle coefficient of 0 would be functionally equivalent to discarding the rotation data of the minutiae and matching the position data with a 3D ICP matcher. The optimal coefficient values for all matches used in the experiment are non-zero, which indicates that our matcher offers an improvement over a standard ICP implementation. The parabolic shape of the graph is similar in all experiments.

The nature of an OCT scanner ensures that the fingerprints will always be partially pre-aligned. Ignoring severe user error, a finger will never be inserted upside down or flipped around, but will always be translated and rotated within a small range. This means that an alignment step does not need to be performed, which saves processing time. Furthermore, the FICP matcher can be configured to only rotate and translate within a certain range, which eliminates severe errors in matching.

Figure 4 shows the results of the two 3D feature types. The composite feature dominates the 3D minutiae, i.e. it outperforms the other both in terms of sensitivity and specificity.

The mean matching times for the two feature types are similar. 3D minutiae have a 95% confidence interval of  $32.0 \pm 0.349$  (1.1%) milliseconds, whereas the composite feature is  $28.7 \pm 0.333$  (1.2%). These times are also very similar to the 2D minutiae FICP matcher, suggesting that feature complexity does not significantly decrease matching performance. The time to extract mean local intensities is negligible: searching an organised point cloud is  $O(1)$  and calculating the mean of an array is  $O(m)$ , for very small values of  $m$ . A tiny increment in extraction time leads to a significant improvement in matching performance.

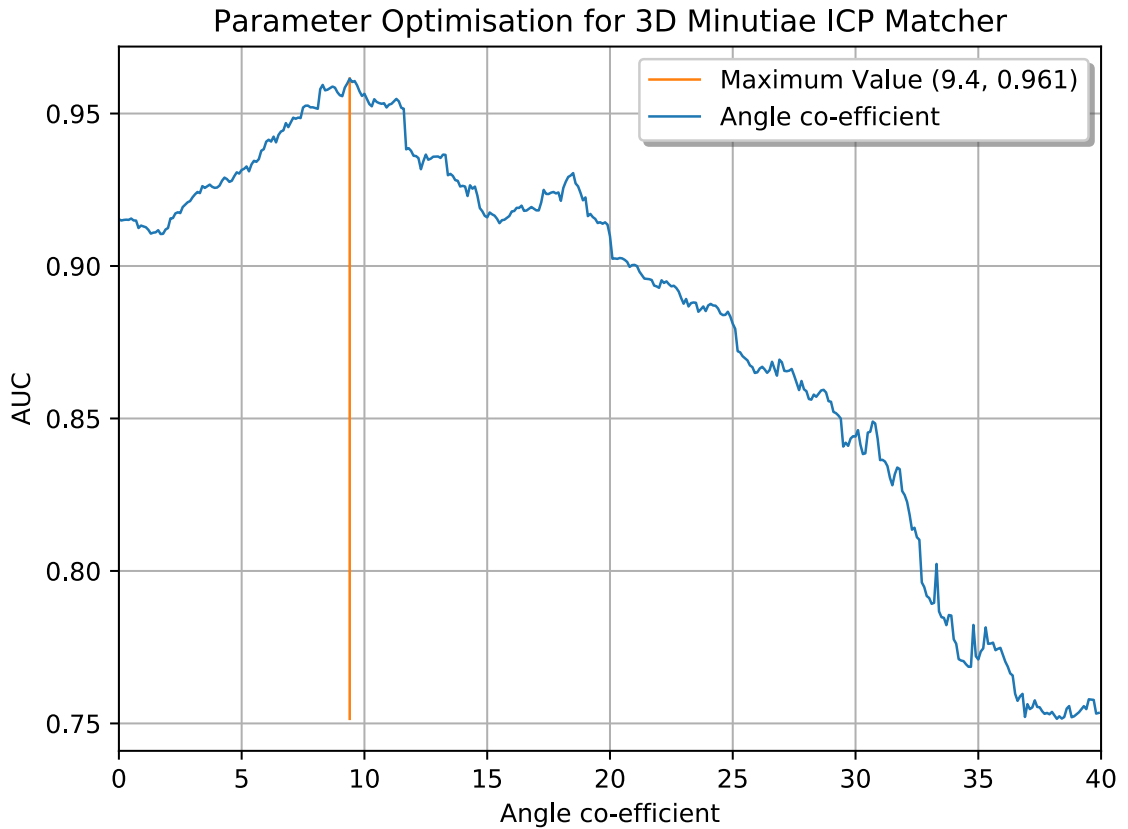


Fig. 3. The graph illustrates the output of the parameter optimisation performed in the initialisation of this experiment for 3D minutiae. The graph shows that the maxima for the angle co-efficient is a non-zero value, demonstrating that FICP is an improvement over Cartesian only ICP.

Our 3D minutiae matcher is highly sensitive to angular noise, as the algorithm parameters are optimised to a specific data set; angular noise might cause the nearest neighbour function to match the wrong minutiae.

#### 5.4 Resilience to Poor Data

Our final experiment addresses the question of how many points an FICP matcher might require to make a reliable match. The 3D minutiae dataset was used for this purpose, to demonstrate the matchers capabilities with modern 3D features.

Pairs of scans were chosen which had a minimum of 20 minutiae in each pair, then minutiae were randomly discarded until each pair had exactly 20 minutiae. Matching was performed and the AUC and Equal Error Rate (EER) was recorded. A single minutia was discarded and the measurements were recorded. This process was repeated until there were three minutiae left in the source scan. The number of minutiae in the reference scans were kept constant. This process emulated a possible security scenario, where there will be a high-quality reference scan on the database and a variable quality scan coming from a scanner or a latent fingerprint.

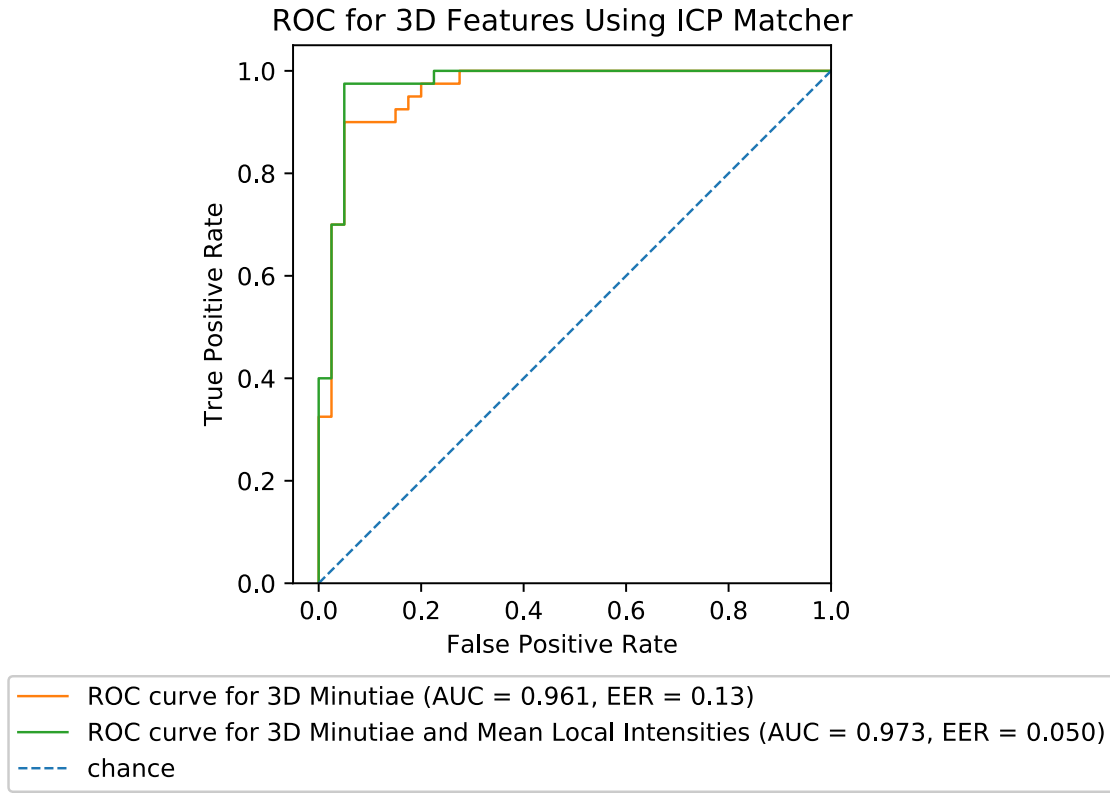


Fig. 4. The FICP matcher’s ROCs for two different 3D features are plotted.

The results of this experiment are shown in Figure 5. There is an approximately linear relationship between the number of minutiae and the AUC. For minutiae in the range [6..20] the AUC is fairly consistent at approximately 0.85, due to the shallow slope of -0.0083. This result shows that FICP is still useful in low-quality scans, with up to a minimum of 6 minutiae. Below 4 minutiae, the matcher performs as well as chance.

## 6 CONCLUSION AND FUTURE WORK

We demonstrated that ICP, an established point alignment algorithm, can serve as the basis for a minutia matching algorithm. We applied our FICP matcher to generated 2D minutiae and real 3D minutiae, thereby demonstrating its superior performance in terms of most matching metrics, when compared to *Bozorth3*, a well-established baseline. Our FICP matcher has a number of significant advantages: (1) it is based on an open source algorithm and is simple to implement; (2) ICP is designed for point alignment and therefore requires no additional alignment step regarding fingerprints; and (3) it is easily adaptable to different feature types, with nominal performance penalty for more complex features.

FICP enables high accuracy matches to be made in both 2D and 3D using simple, fast to extract features. Our custom metrics have been shown to improve the accuracy of ICP.

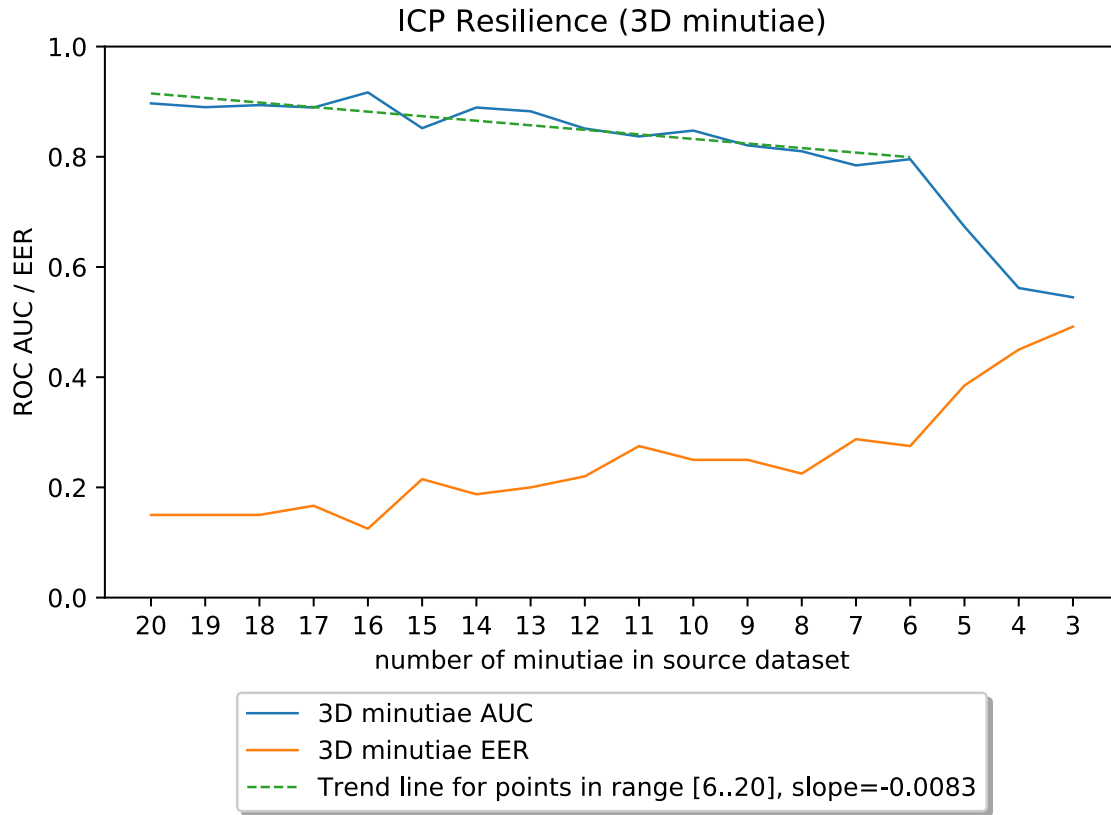


Fig. 5. The graph illustrates the ROC's AUC and EER for diminishing numbers of minutiae in the source scan. The matching accuracy remains quite high, but benefits from more minutiae. This is for 3D minutiae extracted from the OCT dataset.

We have not optimised our FICP matcher for speed: it is slightly slower than *Bozorth3*. However, there is scope for dramatic improvement as ICP is an embarrassingly parallel algorithm. Parallelised ICP implementations exist, such as Point Cloud Library [11], which this system could be adapted to.

The FICP would benefit from testing with a larger and more diverse 3D minutiae dataset. The lack of available 3D fingerprint data limited the testing we could undertake.

#### ACKNOWLEDGMENTS

The authors would like to acknowledge a 1 year studentship from the CSIR, South Africa, that helped to support this work.

#### REFERENCES

- [1] Paul J. Besl and Neil D. McKay. 1992. A Method for Registration of 3-D Shapes. *IEEE Transactions on Pattern Analysis and Machine Intelligence* 14, 2 (1992), 239–256. <https://doi.org/10.1109/34.121791>
- [2] Partha Bhowmick and Bhargab B. Bhattacharya. 2004. Approximate fingerprint matching using Kd-tree. In *Proceedings - International Conference on Pattern Recognition*, Vol. 1. IEEE, 544–547. <https://doi.org/10.1109/ICPR.2004.1334194>
- [3] Raffaele Cappelli. 2015. *SFinGe*. Springer US, Boston, MA, 1360–1367. [https://doi.org/10.1007/978-1-4899-7488-4\\_8](https://doi.org/10.1007/978-1-4899-7488-4_8)

- [4] Luke Nicholas Darlow and James Connan. 2015. Efficient internal and surface fingerprint extraction and blending using optical coherence tomography. *Journal of Electronic Imaging* 54, 31 (2015), 9258–9268.
- [5] Luke Nicholas Darlow, James Connan, and Ann Singh. 2016. Performance analysis of a Hybrid fingerprint extracted from optical coherence tomography fingertip scans. In *2016 International Conference on Biometrics (ICB)*. IEEE, 1–8. <https://doi.org/10.1109/ICB.2016.7550045>
- [6] David Huang, Eric A Swanson, Charles P Lin, Joel S Schuman, William G Stinson, Warren Chang, Michael R Hee, Thomas Flotte, Kenton Gregory, and Carmen A Puliafito. 1991. Optical coherence tomography. *Science (New York, N.Y.)* 254, 5035 (1991), 1178–1181.
- [7] Du Q Huynh. 2009. Metrics for 3D rotations: Comparison and analysis. *Journal of Mathematical Imaging and Vision* 35, 2 (2009), 155–164. <https://doi.org/10.1007/s10851-009-0161-2>
- [8] Sanghoon Kim, Michael Crose, Brian Cox, William Brown, and Adam Wax. 2018. Design and implementation of a low-cost, portable OCT system. In *Optics InfoBase Conference Papers*, Vol. Part F90-O. 1232. <https://doi.org/10.1364/OTS.2018.OF3D.7>
- [9] Ajay Kumar and Cyril Kwong. 2015. Towards contactless, low-cost and accurate 3D fingerprint identification. *IEEE Transactions on Pattern Analysis and Machine Intelligence* 37, 3 (2015), 681–696. <https://doi.org/10.1109/TPAMI.2014.2339818>
- [10] Soumyadip Rakshit and Donald M Monroe. 2006. Effects of sampling and compression on human iris verification. In *2006 IEEE International Conference on Acoustics Speech and Signal Processing Proceedings*, Vol. 2. IEEE, II–II.
- [11] Radu Bogdan Rusu and Steve Cousins. 2011. 3D is here: Point Cloud Library (PCL). In *Proceedings - IEEE International Conference on Robotics and Automation*. 1 – 4. <https://doi.org/10.1109/ICRA.2011.5980567>
- [12] Craig I Watson, Michael D Garris, Elham Tabassi, Charles L Wilson, R Michael McCabe, and Stanley Janet. 2004. User’s guide to NIST fingerprint image software 2 (NFIS2). *National Institute of Standards and Technology* (2004).